Black hole spectroscopy: Systematic errors and ringdown energy estimates

Vishal Baibhav,[1,*] Emanuele Berti,[1,2,†] Vitor Cardoso,[2,3,‡] and Gaurav Khanna[4,§]

[1]*Department of Physics and Astronomy, University of Mississippi, University, Mississippi 38677, USA*
[2]*CENTRA, Departamento de Física, Instituto Superior Técnico, Universidade de Lisboa, Avenida Rovisco Pais 1, 1049 Lisboa, Portugal*
[3]*Perimeter Institute for Theoretical Physics, Waterloo, Ontario N2L 2Y5, Canada*
[4]*Department of Physics and Center for Scientific Computing and Visualization Research, University of Massachusetts Dartmouth, North Dartmouth, Massachusetts 02747, USA*

(Received 5 October 2017; published 28 February 2018)

The relaxation of a distorted black hole to its final state provides important tests of general relativity within the reach of current and upcoming gravitational wave facilities. In black hole perturbation theory, this phase consists of a simple linear superposition of exponentially damped sinusoids (the quasinormal modes) and of a power-law tail. How many quasinormal modes are necessary to describe waveforms with a prescribed precision? What error do we incur by only including quasinormal modes, and not tails? What other systematic effects are present in current state-of-the-art numerical waveforms? These issues, which are basic to testing fundamental physics with distorted black holes, have hardly been addressed in the literature. We use numerical relativity waveforms and accurate evolutions within black hole perturbation theory to provide some answers. We show that (i) a determination of the fundamental $l = m = 2$ quasinormal frequencies and damping times to within 1% or better requires the inclusion of at least the first overtone, and preferably of the first two or three overtones; (ii) a determination of the black hole mass and spin with precision better than 1% requires the inclusion of at least two quasinormal modes for any given angular harmonic mode (ℓ, m). We also improve on previous estimates and fits for the ringdown energy radiated in the various multipoles. These results are important to quantify theoretical (as opposed to instrumental) limits in parameter estimation accuracy and tests of general relativity allowed by ringdown measurements with high signal-to-noise ratio gravitational wave detectors.

DOI: 10.1103/PhysRevD.97.044048

I. INTRODUCTION

The historic LIGO gravitational wave (GW) detections of binary black hole (BH) mergers [1–4] ushered in a new era in astronomy. The growing network of Earth-based interferometers and the future space-based detector LISA will probe the nature of compact objects and test general relativity (GR) in unprecedented ways [5–9]. One of the most interesting prospects is the possibility to use GW observations to measure the quasinormal mode (QNM) oscillation frequencies of binary BH merger remnants. In GR, these oscillation frequencies depend only on the remnant BH mass and spin, so these measurements can identify Kerr BHs just like atomic spectra identify atomic elements. This idea is often referred to as "BH spectroscopy" [10–13]. In the context of modified theories of gravity, QNM frequencies would inform us on possible corrections to GR and allow us to constrain specific theories [14,15]. In other words, the payoff of BH spectroscopy is significant not only as a tool to test GR [16,17], but also as a tool to quantify the presence of event horizons in the spacetime (by looking, for instance, for "echoes" in the relaxation stage [18–21]).

In practice, there are two main obstacles to measuring multiple QNM frequencies (i.e., to identifying multiple spectral lines). The first is of a technological nature and relates to the fact that rather large signal-to-noise ratios (SNRs) are required [22]. Recent estimates suggest that most *individual* binary BH mergers detected by LISA could be used to do BH spectroscopy, but significant technological improvements are necessary for Earth-based detectors to achieve the necessary SNR [23,24]. However the sensitivity of upcoming detectors is constantly improving, and there are good reasons to believe that this issue will eventually be resolved. The second challenge concerns systematic effects which might be unaccounted for in our current theoretical or numerical understanding of the waveforms. For example, it is well-known that (even at the level of linearized perturbation theory) the late-time decay of BH fluctuations is not exponential but polynomial [13,25]. Thus, one must question the validity of exponentially damped sinusoids as a description of

*vbaibhav@go.olemiss.edu
†eberti@olemiss.edu
‡vitor.cardoso@ist.utl.pt
§gkhanna@umassd.edu

the late-time GW signal (see e.g. recent work by Thrane *et al.*, who claimed that spectroscopy will not be possible even in the infinite SNR limit [26]). When does the exponential (QNM) falloff give way to the polynomial tail? Are nonlinearities important, and how do they affect the simple linearized predictions?

There are very few studies of the accuracy achievable in extracting QNM frequencies from numerical simulations. Some of these studies pointed out that the accuracy of numerical waveforms may be limited by gauge choices or wave extraction techniques [27,28]. Therefore we ask: what is the systematic deviation between BH perturbation theory predictions and the QNM frequencies extracted from numerical simulations? In other words, what is the size of systematic errors in the extraction of QNM frequencies from current state-of-the-art numerical simulations? These questions are of paramount importance for any claims about independent BH mass and spin extraction using ringdown waveforms, and for any ringdown-based tests of GR.

We address these questions using public catalogs of numerical relativity simulations (focusing on the Simulating eXtreme Spacetimes (SXS) gravitational waveform database [29]), as well as extreme mass-ratio waveforms produced using the Kerr time-domain perturbative code written by one of us [30,31].

One of the main results of our analysis, validating a multitude of studies in the past decade or so, is that a "pure ringdown" stage does not exist *per se*, detached from the rest of the waveform. In other words, the full glory and complexity of GR must be accounted for when extracting physics. Nevertheless, the notion of ringdown can be useful in the context of simple, independent checks on the physics. We have in mind, for instance, ringdown-based tests of the no-hair theorem or constraints on modified theories of gravity. Accurate models of the amplitude and phase of each QNM are necessary to perform such tests. In fact, these quantities are also crucial to alleviate the problem of low SNRs in individual events by combining posterior probability densities from multiple detections [32] or via coherent stacking [33]. At the moment, our ability to do coherent stacking is limited by the theoretical understanding of ringdown: stacking requires phase alignment between different angular components of the radiation, which can only be achieved through a better understanding of the excitation and starting times of QNMs [34–38]. Most early studies of QNM excitation relied on the evolution of simple initial data (e.g. Gaussian wave packets) in the Kerr background [39,40]. After the 2005 numerical relativity breakthrough, some authors investigated QNM excitation in the merger of nonspinning BHs [41–44], but to this day there is little published work on spinning mergers (with the notable exception of Ref. [45]). In this work we use numerical relativity simulations to fit the energy of the modes for spin-aligned binaries, thus alleviating some of the difficulties inherent in stacking signals for BH spectroscopy.

II. SYSTEMATIC ERRORS IN EXTRACTING QUASINORMAL MODE FREQUENCIES

In the ringdown phase the radiation is a superposition of damped sinusoids with complex frequencies $\omega^{\ell mn}$ parametrized by three integers: the spin-weighted spheroidal harmonic indices (ℓ, m) and an "overtone index" n, which sorts the frequencies by their decay time (the fundamental mode $n = 0$ has the smallest imaginary part and the longest decay time). The complex Penrose scalar Ψ_4 (and the strain h) can be expanded as

$$r\Psi_4^{\ell m} = \Theta(t - t_0^{\ell m}) \sum_{n=1}^{N} B^{\ell mn} \exp\left[\mathrm{i}(\omega^{\ell mn}(t - t_0^{\ell m}) + \phi^{\ell mn})\right], \tag{1}$$

where $\Theta(x)$ is the Heaviside function, $\omega^{\ell mn} = \omega_{\mathrm{r}}^{\ell mn} + \mathrm{i}\omega_{\mathrm{i}}^{\ell mn}$ and $t_0^{\ell m}$ is the so-called "starting time" of ringdown for the given (ℓ, m). Early studies used least-squares fits to extract QNM frequencies from nonspinning binary BH merger simulations [41]. Other fitting procedures were proposed, but yield very similar results [28,42,46]. Therefore, for simplicity, we will use a simple least-squares fit. For illustration, we consider nonspinning SXS waveforms with mass ratios $q = 1$ (SXS:BBH:0180) and $q = 3$ (SXS:BBH:0183), as well as waveforms for point particles falling into a nonrotating BH.

For point particle evolutions we fit the strain h. When considering the SXS comparable-mass merger waveforms we use the Penrose scalar, as it is known to yield slightly better QNM fits [27,41], but we checked that our main conclusions would remain valid had we used the strain h instead. For the multipolar components $(\ell, m) = (2, 2)$, (3,3) and (2,1), that usually dominate the radiation, we use waveforms extrapolated to infinite extraction radius using a second-order polynomial (as reported by the SXS Collaboration, higher-order polynomials could yield noisy results close to the merger). For the (4,4) and higher-order multipoles we found that the ringdown part of the waveform does not converge with extraction radius for a large number of simulations. Furthermore, the largest extraction radii listed in the SXS catalog are different for different simulations, so they cannot be compared directly. We only used waveforms for which the higher-order multipoles seem to converge, finding the EMOP energy as a function of extraction radius, and then comparing all energies (whether computed by interpolation or extrapolation) at an extraction radius of $500M$.

The fits are performed in two different ways in order to address different aspects of the systematic error analysis:

(i) How accurately can we determine the ringdown frequencies themselves, without assuming any (no-hair theorem enforced) relation between the frequencies?

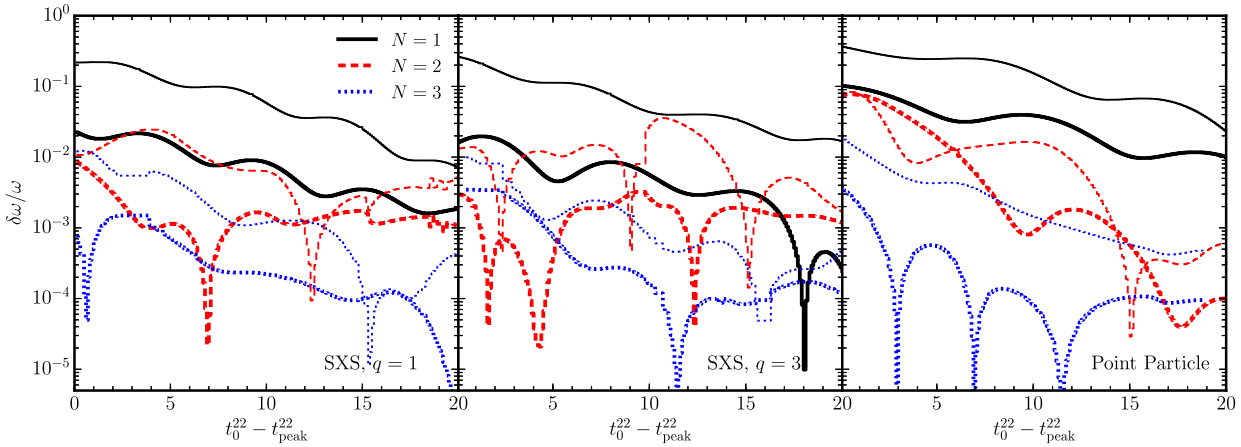

FIG. 1. Fractional errors $\delta\omega_{\rm r}/\omega_{\rm r}$ (thick lines) and $\delta\omega_{\rm i}/\omega_{\rm i}$ (thin lines) between the fundamental $\ell = m = 2$ QNM frequencies computed from BH perturbation theory and those obtained by fitting N overtones to numerical waveforms according to method (i) (see text). Left: SXS waveforms, $q = 1$; middle: SXS waveforms, $q = 3$; right: point-particle waveforms. Here $t_{\rm peak}^{22}$ is the time at which the amplitude of the $l = m = 2$ mode is maximum, and time is measured in units of $c^3/(GM)$.

To answer this question we assume that ($\omega_{\rm r}^{\ell mn}$, $\omega_{\rm i}^{\ell mn}$, $B^{\ell mn}$, $\phi^{\ell mn}$) in Eq. (1) are all unknown, so we have a total of $4N$ fitting coefficients for an N-mode fit. Then we look at the relative error between the real and imaginary part of the fundamental QNM (as derived from the fit) and the predictions from BH perturbation theory [12,13]. This fitting procedure does not enforce the fact that, in GR, QNM frequencies are uniquely determined by the BH mass and spin [12,13]. Systematic errors computed in this way can be seen as lower bounds on how much any given modified theory must modify ringdown frequencies to be experimentally resolvable from GR.

The results are shown in Fig. 1. BHs are poor oscillators, so $\omega_{\rm r}$ is always easier to determine than $\omega_{\rm i}$, and $\delta\omega_{\rm r}/\omega_{\rm r}$ is typically an order of magnitude smaller than $\delta\omega_{\rm i}/\omega_{\rm i}$. Furthermore, Fig. 1 shows that adding overtones generally reduces the systematic error in $\omega_{\rm r}$ and $\omega_{\rm i}$ for all mass ratios. For SXS waveforms we found that including the $N = 4$ mode would not further improve the agreement, while for quasicircular inspirals of point particles into nonrotating BHs $\delta\omega_{\rm r}/\omega_{\rm r}$ and $\delta\omega_{\rm i}/\omega_{\rm i}$ decreases to $\sim 10^{-4}$ and 10^{-3}, respectively.

(ii) How accurately can we determine the remnant's mass and spin from ringdown frequencies, assuming that GR is correct?

To answer this question we still consider ($B_{lm}^{(j)}$, $\phi_{lm}^{(j)}$) as free parameters, but now we enforce the condition that the QNM frequencies $\omega_{\rm r,i}^{\ell mn}$ must be functions of the remnant BH mass $M_{\rm f}$ and dimensionless spin $a_{\rm f}$, so we have only $2N + 2$ fitting coefficients. As shown in Fig. 2, the accuracy in determining both mass and spin is comparable to the accuracy in the poorest determined quantity (i.e., $\omega_{\rm i}$). The trend is the same as in Fig. 1, and errors decrease as we include more overtones.

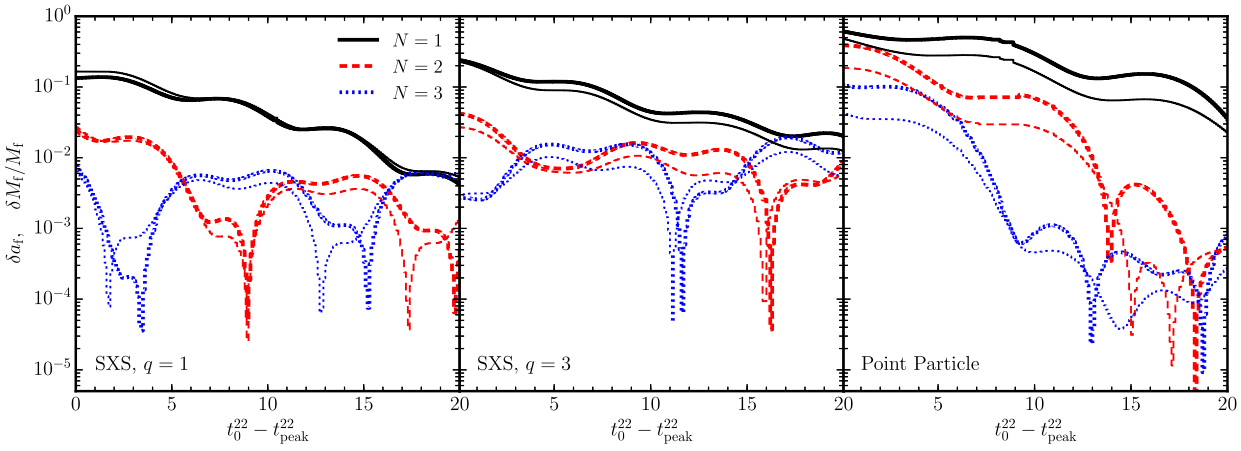

FIG. 2. Error in the spin $\delta a_{\rm f}$ (thick lines) and fractional error in the mass $\delta M_{\rm f}/M_{\rm f}$ (thin lines) estimated by fitting N QNMs with $\ell = m = 2$ according to method (ii) (see text). Left: SXS waveforms, $q = 1$; middle: SXS waveforms, $q = 3$; right: point-particle waveforms. Here $t_{\rm peak}^{22}$ is the time at which the amplitude of the $l = m = 2$ mode is maximum, and time is measured in units of $c^3/(GM)$.

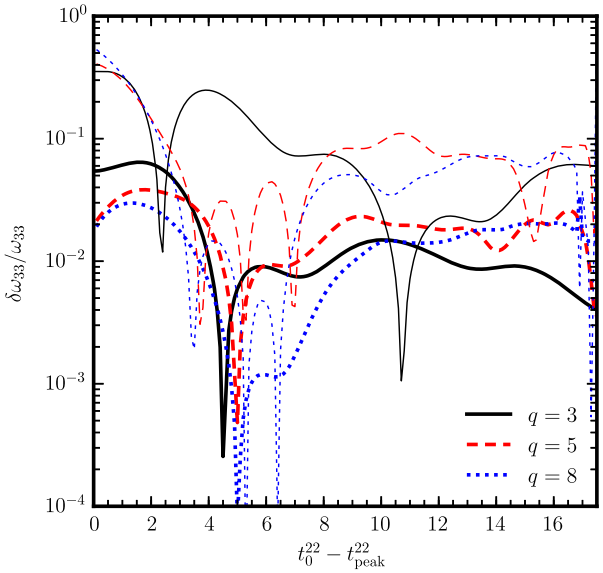

FIG. 3. This figure shows how (3,3) modes contaminate the (2,2) components of unequal-mass BH mergers in the SXS waveforms. We fit the (2,2) mode using a 3-mode fit and method (i) in the text. Then we plot the fractional errors $\delta\omega_{\rm r}/\omega_{\rm r}$ (thick lines) and $\delta\omega_{\rm i}/\omega_{\rm i}$ (thin lines) with respect to the fundamental $\ell = m = 3$ QNM frequencies from BH perturbation theory. This plot used the simulations labeled as SXS:BBH:0183 for $q = 3$, SXS:BBH:0056 for $q = 5$ and SXS:BBH:0063 for $q = 8$.

The results in Figs. 1 and 2 disprove the claim of [26] that large-SNR detections cannot be used to perform BH spectroscopy, but they also show that the relative error between quantities computed in BH perturbation theory and those extracted from numerical simulations currently saturates at $\sim 10^{-3}$. This "saturation effect" is less problematic for the quasicircular inspiral of point particles into Schwarzschild BHs, where relative errors can be reduced by approximately 1 order of magnitude (we get worse agreement for point particles falling into rotating BHs, where spherical-spheroidal mode mixing [41,47–49] must be taken into account).

This observation has an important implication: *further numerical or theoretical work is required to reduce systematic errors for comparable-mass binary BH mergers in the LISA band*, that may have SNRs $\sim 10^3$ or higher [50,51].

The saturation discussed above may be related to an undesired feature of SXS waveforms. It was already noted in [28] that the $\ell = m = 2$ component of Ψ_4 in the SXS simulations contains a spurious decaying mode corresponding to the fundamental $\ell = m = 4$ QNMs for $q = 1$. We confirm their finding. Furthermore, as we show in Fig. 3, a multimode fit of *unequal-mass* waveforms shows the presence of a spurious frequency that matches quite well the fundamental QNM with $\ell = m = 3$.

These spurious modes seem to be present only in the SXS simulations. We did not find them in the public catalog of waveforms from the Georgia Tech group [52], nor in our own point-particle waveforms. Understanding the origin of these modes is beyond the scope of this work. We speculate that they may be gauge or wave extraction artifacts, but they are unlikely to come from spherical-spheroidal mode mixing, which only mixes components with the same m and different ℓ's [41,47–49]. Whatever their origin, these spurious modes must be understood if we want to control systematics at the level required to do BH spectroscopy with LISA.

The sharp local minima in Figs. 1, 2 and 3 suggest that the QNM frequencies (and consequently, the remnant spin and mass) extracted from the ringdown oscillate about their "true" values. We suspect that this is purely due to systematics, but we can not rule out nonlinear effects.

III. RINGDOWN ENERGIES AND STARTING TIMES

An important prerequisite to perform BH spectroscopy (whether via single detections or by stacking) is to quantify the excitation of QNMs and to provide a definition of their starting times which is suitable for data analysis purposes. Quite remarkably, we are aware of only one paper that tried to quantify QNM excitation for spinning binaries [43]. Here we improve on the results of [43] by (i) using newer and more accurate simulations from the SXS catalog and (ii) implementing a better criterion to determine *simultaneously* the energy (or relative amplitude) of different ringdown modes, as well as their starting times.

There is no unique, unambiguous way of defining such a starting time, because ringdown is only an intermediate part of the full signal resulting from the merger dynamics of the two-body system. Nevertheless, a physically sensible, detector-independent criterion is to decompose the full waveform into components "parallel" and "perpendicular" to the QNM. The ringdown starting time is defined as the point where the energy "parallel to the QNM" is maximized. Nollert, who introduced this concept, called this the "energy maximized orthogonal projection" (EMOP) [36]. Nollert's EMOP criterion can be interpreted in data analysis terms as answering the following question: given a single-mode QNM template, what starting time would maximize the ringdown energy in the infinite-SNR limit? This question is clearly relevant to GW data analysis, and it provides a "unique" definition of the starting time that does not depend on the detector's sensitivity. Note that maximizing the energy in the fundamental mode is not the same as minimizing the errors in (say) the remnant's mass and spin. A ringdown waveform starting at time t_0 has the form

$$h_{\rm QNM} = h^{+}_{\rm QNM} + i h^{\times}_{\rm QNM} = \Theta(t - t_0) \exp\left[\mathrm{i}(\omega t + \phi)\right].$$

Given the complex strain $h = h^{+} + i h^{\times}$ from numerical relativity, the energy "parallel to the QNM" $h_{\rm QNM}$ is

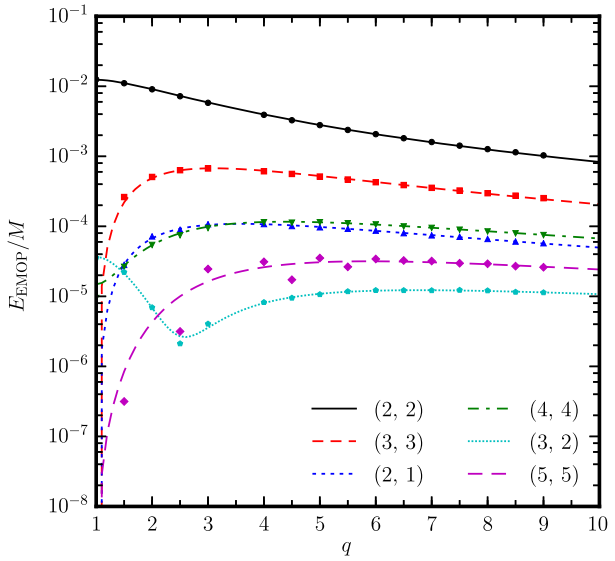

FIG. 4. EMOP energies as a function of mass ratio for nonspinning binaries in the SXS catalog. The anomalous behavior of the (3,2) mode is due to spherical-spheroidal mode mixing [41,47–49]: the contamination of the (2,2) mode observed in the (3,2) mode is more prominent for comparable mass ratios.

$$E_{\parallel} = \frac{1}{8\pi}\frac{|\int_{t_0} \dot{h}\dot{h}^*_{\rm QNM} dt|^2}{\int_{t_0} \dot{h}_{\rm QNM}\dot{h}^*_{\rm QNM} dt} = \frac{\omega_{\rm i}|\int_{t_0} \dot{h}\dot{h}^*_{\rm QNM} dt|^2}{4\pi(\omega_{\rm i}^2+\omega_{\rm r}^2)}, \quad (2)$$

where in the second equality we have explicitly evaluated the integral in the denominator. The ringdown starting time is defined as the lower limit of integration t_0 such that $E_{\parallel}$ in Eq. (2) is maximum, and the EMOP energy is $E_{\rm EMOP} = \max_{t_0}(E_{\parallel})$.

Equation (2) is an improvement over the definition used in [42], where we first computed the EMOP energy separately for the plus and cross polarizations, and then averaged the starting time from the two polarizations. Furthermore $E_{\parallel}$ is independent of phase rotations in either the numerical waveform ($h \to he^{i\theta}$) or in the QNM ($h_{\rm QNM} \to h_{\rm QNM}e^{i\phi}$). EMOP energies computed from the SXS waveforms for nonspinning binary mergers are shown in Fig. 4.

For binaries with aligned spins, a good fit to the EMOP energy in the first few dominant (ℓ, m) modes is

$$E_{\ell m} = \begin{cases} \eta^2(\mathcal{A}^0_{\ell m} + \mathcal{A}^{\rm spin}_{\ell m})^2, & {\rm even}\, m, \\ \eta^2(\sqrt{1-4\eta}\mathcal{A}^0_{\ell m} + \mathcal{A}^{\rm spin}_{\ell m})^2, & {\rm odd}\, m, \end{cases} \quad (3)$$

where the nonspinning contribution $\mathcal{A}^0_{\ell m}$ is well fitted by

$$\mathcal{A}^0_{\ell m} = a^0_{\ell m} + b^0_{\ell m}\eta, \quad (\ell, m) = (2,2), (3,3), (2,1),$$
$$\mathcal{A}^0_{\ell m} = a^0_{\ell m} + b^0_{\ell m}\eta + c^0_{\ell m}\eta^2, \quad (\ell, m) = (3,2), (4,4), (5,5),$$

and $\eta = q/(1+q)^2$ is the symmetric mass ratio. The contribution from the spins $\mathcal{A}^{\rm spin}_{\ell m}$ can be written in terms of the symmetric and asymmetric effective spins

$$\chi_{\pm} \equiv \frac{m_1\chi_1 \pm m_2\chi_2}{M}, \quad (4)$$

where χ_1 and χ_2 are the dimensionless spins of the two BHs, and $\chi_+ = \chi_{\rm eff}$ (the "effective spin" parameter best measured by LIGO, which is conserved in post-Newtonian evolutions at 2PN order [53–56]).

We use the post-Newtonian inspired fits [57,58]

$$\mathcal{A}^{\rm spin}_{22} = \eta\chi_+\left(a^{\rm s}_{22} + \frac{b^{\rm s}_{22}}{q} + c^{\rm s}_{22}q + d^{\rm s}_{22}q^2\right) + e^{\rm s}_{22}\delta\chi_-,$$
$$\mathcal{A}^{\rm spin}_{33} = \eta\chi_-\left(a^{\rm s}_{33} + \frac{b^{\rm s}_{33}}{q} + c^{\rm s}_{33}q\right) + d^{\rm s}_{33}\delta\chi_+,$$
$$\mathcal{A}^{\rm spin}_{21} = a^{\rm s}_{21}\chi_-,$$
$$\mathcal{A}^{\rm spin}_{44} = \eta\chi_+\left(\frac{a^{\rm s}_{44}}{q} + b^{\rm s}_{44}q\right) + \delta\eta\chi_-\left(c^{\rm s}_{44} + \frac{d^{\rm s}_{44}}{q} + e^{\rm s}_{44}q\right), \quad (5)$$

where $\delta = \sqrt{1-4\eta} = (q-1)/(q+1)$. The fitting coefficients, along with the mean and maximum percentage errors of each fit, are listed in Table I. The dependence of the EMOP energy on spins is illustrated in Fig. 5 for simulations with mass ratio $q = 2$.

TABLE I. Fitting coefficients for the EMOP energy, along with the corresponding errors. A superscript "0" corresponds to the nonspinning contribution, while "s" denotes the spin-dependent contributions. Since poorly excited modes tend to be dominated by numerical noise, we have only considered modes with $E_{\rm EMOP} \geq 10^{-4}M$. We also dropped the (4,4) mode data from some simulations where the EMOP energy did not converge as we increase the wave extraction radius.

Modes	a^0	b^0	c^0	a^s	b^s	c^s	d^s	e^s	Max. error (%)	Mean error (%)
(2,2)	0.303	0.571	0	−0.07	0.255	0.189	−0.013	0.084	3.63	0.64
(3,3)	0.157	0.671	0	0.163	−0.187	0.021	0.073	0	11.24	2.32
(2,1)	0.099	0.06	0	−0.067	0	0	0	0	9.54	2.01
(4,4)	0.122	−0.188	−0.964	−0.207	0.034	−0.701	1.387	0.122	12.75	1.93

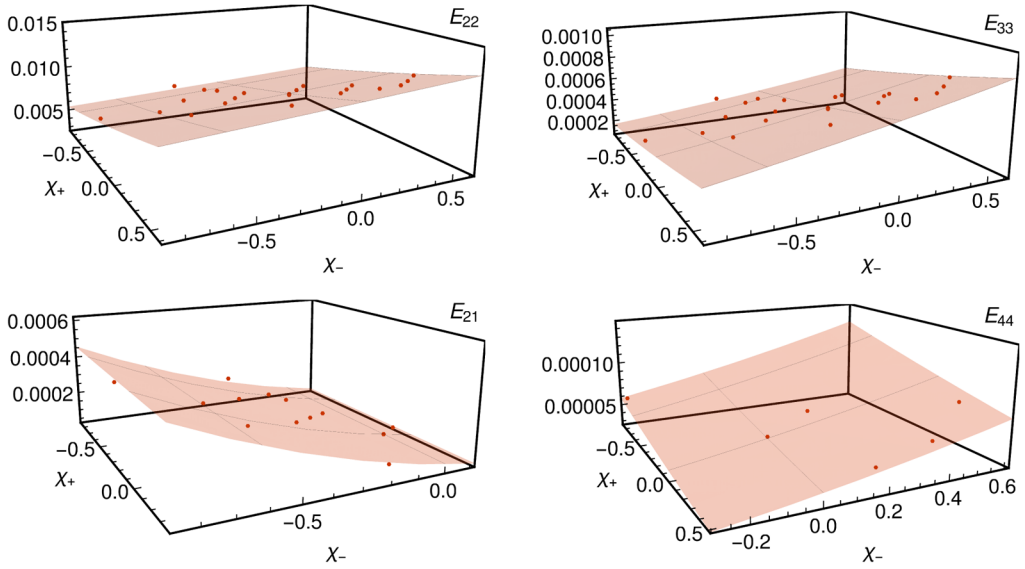

FIG. 5. EMOP energies $E_{\ell m}$ in different (ℓ, m) modes for aligned-spin SXS simulations with $q = 2$ as a function of χ_+ and χ_-, along with the fits given in Eq. (3).

IV. CONCLUSIONS

The recent detection of gravitational waves by the LIGO/Virgo Collaboration makes the prospect of spectroscopic tests of general relativity realistic in the near future. As detectors and data quality improve, a good understanding of the ringdown stage will require an assessment of systematic errors affecting the waveforms. Previous studies bounded environmental and astrophysical effects in BH ringdown waveforms [59]. In this work we started addressing how numerical and/or theoretical limitations affect our ability to perform BH spectroscopy. It is known that the late-time behavior of any BH perturbation should be a power-law decay. Thus, a description using exponentially damped sinusoids must eventually break down.

We showed that no precise tests of GR nor any accurate measurement of BH masses or spins are possible with single-mode templates: two or three modes are necessary.

To facilitate spectroscopic tests (whether in single detections or via stacking) we extended the EMOP calculations of Ref. [42] using the SXS waveforms in the case of (anti)aligned spins. In this preliminary study we neglected subtle issues such as mode mixing, which is known to affect in particular the (3,2) mode [41,48,49]. Further work is required to apply our results in gravitational-wave data analysis [12,32,42,60,61] or to understand how these systematics affect tests general relativity with ringdown, e.g. within the "post-Kerr" framework proposed in [15].

Even after subtracting three or four quasinormal modes, our analysis shows no evidence of power-law tails in the numerical data. This probably means that tails dominate the signal only at very late times, when numerical error is already significant. Notwithstanding, and due to their interesting origin—backscatter off spacetime curvature—the identification of tails in numerical simulations of comparable mass BH mergers is an interesting challenge that should be addressed in future work.

ACKNOWLEDGMENTS

We thank Bangalore Sathyaprakash, K. G. Arun, and Daniel George for useful discussions. V. B. and E. B. are supported by NSF Grants No. PHY-1607130 and No. AST-1716715, and by FCT Contract No. IF/00797/2014/CP1214/CT0012 under the IF2014 Programme. V. C. acknowledges financial support provided under the European Union's H2020 ERC Consolidator Grant "Matter and strong-field gravity: New frontiers in Einstein's theory" Grant No. MaGRaTh–646597. Research at Perimeter Institute is supported by the Government of Canada through Industry Canada and by the Province of Ontario through the Ministry of Economic Development & Innovation. G. K. acknowledges research support from the National Science Foundation Grant No. PHY-1701284) and Air Force Research Laboratory (Grant No. 10-RI-CRADA-09). This project has received funding from the European Union's Horizon 2020 research and innovation programme under the Marie Sklodowska-Curie Grant No. 690904. The authors would like to acknowledge networking support by the COST Action CA16104.

[1] B. P. Abbott *et al.* (Virgo, LIGO Scientific Collaborations), Phys. Rev. Lett. **116**, 061102 (2016).
[2] B. P. Abbott *et al.* (Virgo, LIGO Scientific Collaborations), Phys. Rev. Lett. **116**, 241103 (2016).
[3] B. P. Abbott *et al.* (VIRGO, LIGO Scientific Collaborations), Phys. Rev. Lett. **118**, 221101 (2017).
[4] B. P. Abbott *et al.* (Virgo, LIGO Scientific Collaborations), Phys. Rev. Lett. **119**, 141101 (2017).
[5] B. P. Abbott *et al.* (Virgo, LIGO Scientific Collaborations), Phys. Rev. Lett. **116**, 221101 (2016).
[6] N. Yunes, K. Yagi, and F. Pretorius, Phys. Rev. D **94**, 084002 (2016).
[7] J. R. Gair, M. Vallisneri, S. L. Larson, and J. G. Baker, Living Rev. Relativity **16**, 7 (2013), arXiv:1212.5575.
[8] N. Yunes and X. Siemens, Living Rev. Relativity **16**, 9 (2013), arXiv:1304.3473.
[9] E. Berti *et al.*, Classical Quantum Gravity **32**, 243001 (2015).
[10] S. L. Detweiler, Astrophys. J. **239**, 292 (1980).
[11] O. Dreyer, B. J. Kelly, B. Krishnan, L. S. Finn, D. Garrison, and R. Lopez-Aleman, Classical Quantum Gravity **21**, 787 (2004).
[12] E. Berti, V. Cardoso, and C. M. Will, Phys. Rev. D **73**, 064030 (2006).
[13] E. Berti, V. Cardoso, and A. O. Starinets, Classical Quantum Gravity **26**, 163001 (2009).
[14] J. L. Blázquez-Salcedo, C. F. B. Macedo, V. Cardoso, V. Ferrari, L. Gualtieri, F. S. Khoo, J. Kunz, and P. Pani, Phys. Rev. D **94**, 104024 (2016).
[15] K. Glampedakis, G. Pappas, H. O. Silva, and E. Berti, Phys. Rev. D **96**, 064054 (2017).
[16] V. Cardoso and L. Gualtieri, Classical Quantum Gravity **33**, 174001 (2016).
[17] V. Cardoso and P. Pani, Nat. Astron. **1**, 586 (2017).
[18] V. Cardoso, E. Franzin, and P. Pani, Phys. Rev. Lett. **116**, 171101 (2016); **117**, 089902(E) (2016).
[19] V. Cardoso, S. Hopper, C. F. B. Macedo, C. Palenzuela, and P. Pani, Phys. Rev. D **94**, 084031 (2016).
[20] J. Abedi, H. Dykaar, and N. Afshordi, Phys. Rev. D **96**, 082004 (2017).
[21] Z. Mark, A. Zimmerman, S. M. Du, and Y. Chen, Phys. Rev. D **96**, 084002 (2017).
[22] E. Berti, J. Cardoso, V. Cardoso, and M. Cavaglia, Phys. Rev. D **76**, 104044 (2007).
[23] E. Berti, A. Sesana, E. Barausse, V. Cardoso, and K. Belczynski, Phys. Rev. Lett. **117**, 101102 (2016).
[24] S. Bhagwat, D. A. Brown, and S. W. Ballmer, Phys. Rev. D **94**, 084024 (2016); **95**, 069906(E) (2017).
[25] R. H. Price, Phys. Rev. D **5**, 2419 (1972).
[26] E. Thrane, P. D. Lasky, and Y. Levin, Phys. Rev. D **96**, 102004 (2017).
[27] A. Buonanno, Y. Pan, H. P. Pfeiffer, M. A. Scheel, L. T. Buchman, and L. E. Kidder, Phys. Rev. D **79**, 124028 (2009).
[28] A. Zimmerman and Y. Chen, Phys. Rev. D **84**, 084012 (2011).
[29] A. H. Mroue *et al.*, Phys. Rev. Lett. **111**, 241104 (2013).
[30] P. A. Sundararajan, G. Khanna, and S. A. Hughes, Phys. Rev. D **81**, 104009 (2010).
[31] A. Zenginoglu and G. Khanna, Phys. Rev. X **1**, 021017 (2011).
[32] J. Meidam, M. Agathos, C. Van Den Broeck, J. Veitch, and B. S. Sathyaprakash, Phys. Rev. D **90**, 064009 (2014).
[33] H. Yang, K. Yagi, J. Blackman, L. Lehner, V. Paschalidis, F. Pretorius, and N. Yunes, Phys. Rev. Lett. **118**, 161101 (2017).
[34] N. Andersson, Phys. Rev. D **51**, 353 (1995).
[35] H.-P. Nollert and R. H. Price, J. Math. Phys. (N.Y.) **40**, 980 (1999).
[36] H.-P. Nollert, *Characteristic Oscillations of Black Holes and Neutron Stars: From Mathematical Background to Astrophysical Applications* (Habilitationsschrift Der Fakultat fur Physik der Eberhard-Karls-Universitat, Tubingen, Tubingen, 2000).
[37] E. Berti and V. Cardoso, Phys. Rev. D **74**, 104020 (2006).
[38] Z. Zhang, E. Berti, and V. Cardoso, Phys. Rev. D **88**, 044018 (2013).
[39] W. Krivan, P. Laguna, P. Papadopoulos, and N. Andersson, Phys. Rev. D **56**, 3395 (1997).
[40] E. N. Dorband, E. Berti, P. Diener, E. Schnetter, and M. Tiglio, Phys. Rev. D **74**, 084028 (2006).
[41] A. Buonanno, G. B. Cook, and F. Pretorius, Phys. Rev. D **75**, 124018 (2007).
[42] E. Berti, V. Cardoso, J. A. Gonzalez, U. Sperhake, M. Hannam, S. Husa, and B. Bruegmann, Phys. Rev. D **76**, 064034 (2007).
[43] I. Kamaretsos, M. Hannam, S. Husa, and B. S. Sathyaprakash, Phys. Rev. D **85**, 024018 (2012).
[44] L. London, D. Shoemaker, and J. Healy, Phys. Rev. D **90**, 124032 (2014); **94**, 069902(E) (2016).
[45] I. Kamaretsos, M. Hannam, and B. Sathyaprakash, Phys. Rev. Lett. **109**, 141102 (2012).
[46] E. Berti, V. Cardoso, J. A. Gonzalez, and U. Sperhake, Phys. Rev. D **75**, 124017 (2007).
[47] E. Berti, V. Cardoso, and M. Casals, Phys. Rev. D **73**, 024013 (2006); **73**, 109902(E) (2006).
[48] B. J. Kelly and J. G. Baker, Phys. Rev. D **87**, 084004 (2013).
[49] E. Berti and A. Klein, Phys. Rev. D **90**, 064012 (2014).
[50] P. Amaro-Seoane *et al.*, GW Notes **6**, 4 (2013).
[51] H. Audley *et al.*, arXiv:1702.00786.
[52] K. Jani, J. Healy, J. A. Clark, L. London, P. Laguna, and D. Shoemaker, Classical Quantum Gravity **33**, 204001 (2016).
[53] M. Kesden, U. Sperhake, and E. Berti, Phys. Rev. D **81**, 084054 (2010).
[54] M. Kesden, D. Gerosa, R. O'Shaughnessy, E. Berti, and U. Sperhake, Phys. Rev. Lett. **114**, 081103 (2015).
[55] D. Gerosa, M. Kesden, U. Sperhake, E. Berti, and R. O'Shaughnessy, Phys. Rev. D **92**, 064016 (2015).
[56] D. Gerosa, M. Kesden, R. O'Shaughnessy, A. Klein, E. Berti, U. Sperhake, and D. Trifirò, Phys. Rev. Lett. **115**, 141102 (2015).
[57] E. Barausse and A. Buonanno, Phys. Rev. D **81**, 084024 (2010).
[58] Y. Pan, A. Buonanno, R. Fujita, E. Racine, and H. Tagoshi, Phys. Rev. D **83**, 064003 (2011); **87**, 109901(E) (2013).
[59] E. Barausse, V. Cardoso, and P. Pani, Phys. Rev. D **89**, 104059 (2014).
[60] S. Gossan, J. Veitch, and B. S. Sathyaprakash, Phys. Rev. D **85**, 124056 (2012).
[61] A. Ghosh *et al.*, Phys. Rev. D **94**, 021101 (2016).